Electronic Supporting Information (ESI) for

Synthesis, Photophysical, and Electrochemical Properties of *β*-Substituted Imidazole-Appended Metalloporphyrins and their NLO Application

Sumit Kumar Yadav[a], Albin Kuriakose[b], Shivani Rathi[a], G. Vijaya Prakash[b]* and Muniappan Sankar[a]*

[a]*Department of Chemistry, Indian Institute of Technology Roorkee, Roorkee 247667, India*

[b]*Nanophotonics Lab, Department of Physics, Indian Institute of Technology Delhi, New Delhi 110016, India*

Table of contents		Page No.
	Experimental section	S2
Fig. S1	MALDI-TOF mass spectrum of NiTPP(Phen) with HABA matrix in positive ion mode at 298 K.	S4
Fig. S2	MALDI-TOF mass spectrum of ZnTPP(Phen) with HABA matrix in positive ion mode at 298 K.	S5
Fig. S3	MALDI-TOF mass spectrum of CoTPP(Phen) with HABA matrix in positive ion mode at 298 K.	S5
Fig. S4	MALDI-TOF mass spectrum of CuTPP(Phen) with HABA matrix in positive ion mode at 298 K.	S6
Fig. S5	^{1}H NMR spectrum of NiTPP(Phen) in DMSO-d_6 at 298 K.	S6
Fig. S6	^{1}H NMR spectrum of ZnTPP(Phen) in DMSO-d_6 at 298 K.	S7
Fig. S7	Energy profile depicting frontier molecular orbitals for MTPP(Phen) (M = Co, Ni).	S8
Fig. S8	Ground state optimized geometries showing top views of (a) H_2TPP(Phen), (c) CuTPP(Phen), (e) ZnTPP(Phen) side view (b) of H_2TPP(Phen), (d) CuTPP(Phen), (f) ZnTPP(Phen) (*meso*-phenyl has been removed for clarity in the side view).	S9
Fig. S9	Ground state optimized geometries showing top views of (a) CoTPP(Phen), (c) NiTPP(Phen), side view (b) of CoTPP(Phen), (d)	S9

Experimental section

Instrumentation and Methods

^{1}H NMR spectra were recorded on JEOL ECX 500 MHz using DMSO-d_6 as solvent at 298 K. The photophysical data was recorded on Shimadzu UV-1800 spectrophotometer. MALDI-TOF MS were recorded on Bruker UltrafleXtreme-TN MALDI-TOF spectrometer using HABA as a matrix at 298 K. EPR spectrum was recorded using Bruker BIOSPIN EMXmicro A200 in distilled toluene at 100 K. Spectrum was simulated in the powder phase using WINEPR SimFonia software. Cyclic voltametric studies were carried out in CHI 7044E work station having three electrode assembly consisting of a platinum electrode as a working electrode, a platinum counter electrode, and saturated Ag/AgCl as a reference electrode at 298 K under argon atmosphere in dry CH_2Cl_2.

Z-scan measurements with open aperture (OA) and closed aperture (CA) configurations were conducted utilizing a Ti:Sapphire laser operating at 800 nm, featuring an 84 MHz repetition rate and a pulse duration of 120 fs. The elaborate Z-scan setup is explained elsewhere. A 15 cm convex lens was used where the corresponding Rayleigh length was 2.54 mm and a sample cuvette (quartz) of 1 mm path length. The transmittance signal for each Z movement was acquired using a photodiode linked to the NI-Scope, with the position adjusted by a computer-controlled translation stage.

Experimental Section

General procedure for the synthesis of MTPP(Phen) [M = 2H, Zn(II), Ni(II), Co(II), or Cu(II)] complexes

To a solution of 2-formyl-5,10,15,20-tetraphenylmatallo-porphyrins (MTPPCHO) (0.057 mmol) in distilled chloroform (30 ml), glacial acetic acid (6 ml), (chloroform/acetic acid (5:1)), 1,10-phenonthroline-dione and ammonium acetate (1.14 mmol) were added to the reaction mixture and allowed to reflux at 65°C for 72 hours. After completion (monitored by TLC), the mixture was cooled to room temperature and washed with water (3 × 30 mL) to remove excess acetic acid and ammonium salts. The organic phase was separated, dried over anhydrous Na_2SO_4, and concentrated under reduced pressure to yield a crude solid. Purification was carried out using silica gel column chromatography. A chloroform/methanol mixture (98:2, v/v) was identified as the optimal eluent during purification trials. Elution with this solvent system afforded the *β*-imidazole-appended metalloporphyrins as colored solids in **72–88% yield**.

NiTPP(Phen)

Red solid, yield: 45 mg (88%); UV λmax (ε × 10^{-5} L mol^{-1} cm^{-1}): 423 (5.33), 537 (4.26), 571 (3.96) nm; ^{1}H NMR (500 MHz, DMSO-d_6) (ppm) δ: 12.34 (s, 1H, outer-NH), 8.19 (s, 1H, β-H), 8.16-8.15 (d, 2H, β-H), 7.88-7.84 (m, 5H, β-H), 7.79-5.69 (m, 26 H, Ph-H/Phen-H). MS (MALDI-TOF) (m/z): calctd. 898.233 $[M+H]^+$, found 898.332. Elemental analysis calctd. (%) for $C_{57}H_{34}NiN_8$; C, 76.21; H, 4.07; N, 12.93; found C, 75.33; H, 3.94; N, 12.91

ZnTPP(Phen)

Light green solid, yield: 36 mg (72%); UV λmax (ε × 10^{-5} L mol^{-1} cm^{-1}): 427 (5.24), 523 (3.60), 556 (4.06) nm; ^{1}H NMR (500 MHz, DMSO-d_6) (ppm) δ: 12.64 (s, 1H, outer-NH), 7.99-7.92 (br, 2H, β-H), 7.70-7.47 (m, 5H, β-H), 7.06-6.99 (m, 9H, β-H), 6.82-6.81 (d, 2 H, Phen-H), 6.63-6.58 (m, 10H, β-H/Phen-H), 5.74-5.70 (br, 2H-Phen-H) . MS (MALDI-TOF) (m/z): calctd. 898.233 $[M]^+$, found 898.332. Elemental analysis calctd. (%) for $C_{57}H_{34}ZnN_8$; C, 76.21; H, 3.92; N, 12.58; found C, 76.18; H, 4.01; N, 12.51

CuTPP(Phen) Red solid, yield: 43 mg (87%); UV λmax (ε × 10^{-5} L mol^{-1} cm^{-1}): 424 (5.40), 536 (4.25), 571 (3.85) nm. MS (MALDI-TOF) (m/z): calctd. 898.233 $[M]^+$, found 898.332.

Elemental analysis calctd. (%) for $C_{57}H_{34}CuN_8$; C, 76.39; H, 3.92; N, 12.56; found C, 76.25; H, 3.83; N, 12.49

^{1}H NMR (500 MHz, DMSO-d_6): No well-resolved signals observed due to strong paramagnetic broadening of Cu(II).

CoTPP(Phen)

Red solid, yield: 42 mg (82%); UV λmax (ε × 10^{-5} L mol^{-1} cm^{-1}): 419 (5.28), 530 (4.29), 573 (4.07) nm. MS (MALDI-TOF) (m/z): calctd. 898.233 $[M]^+$, found 898.332. Elemental analysis calctd. (%) for $C_{57}H_{34}CoN_8$; C, 76.91; H, 3.82; N, 12.58; found C, 76.78; H, 3.87; N, 12.53

^{1}H NMR (500 MHz, DMSO-d_6): Paramagnetic Co(II) complex; spectra show extensive broadening, preventing meaningful peak assignment.

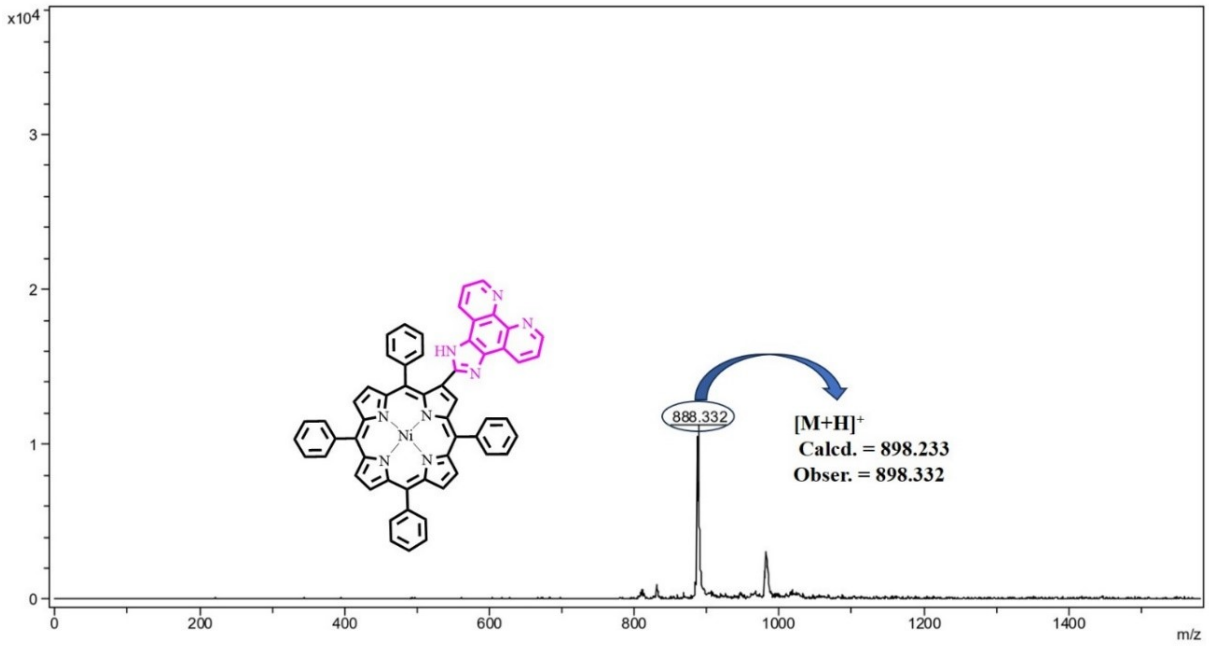

Fig. S1. MALDI-TOF mass spectrum of NiTPP(Phen) with HABA matrix in positive ion mode at 298 K.

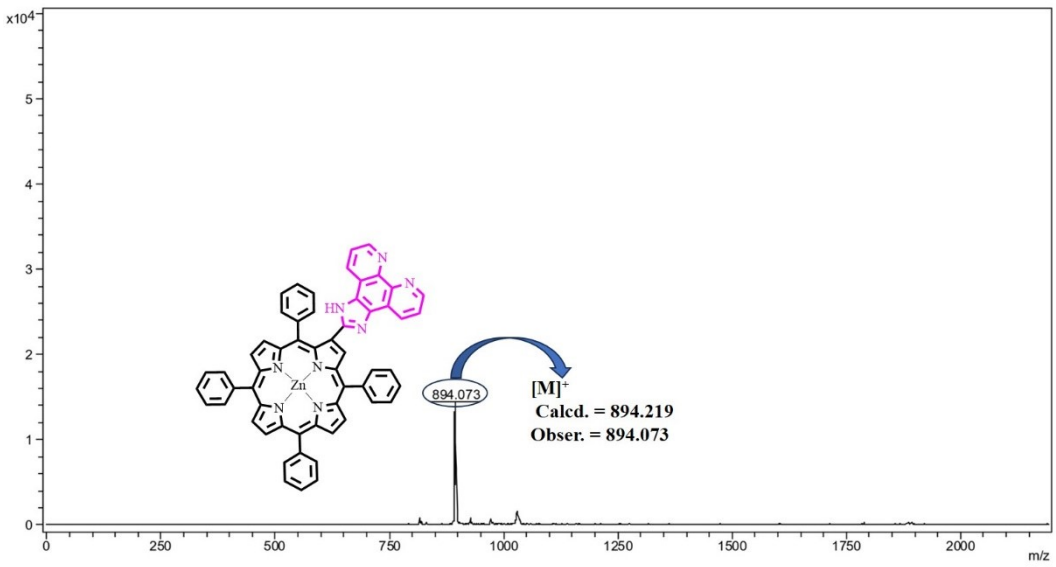

Fig. S2. MALDI-TOF mass spectrum of ZnTPP(Phen) with HABA matrix in positive ion mode at 298 K.

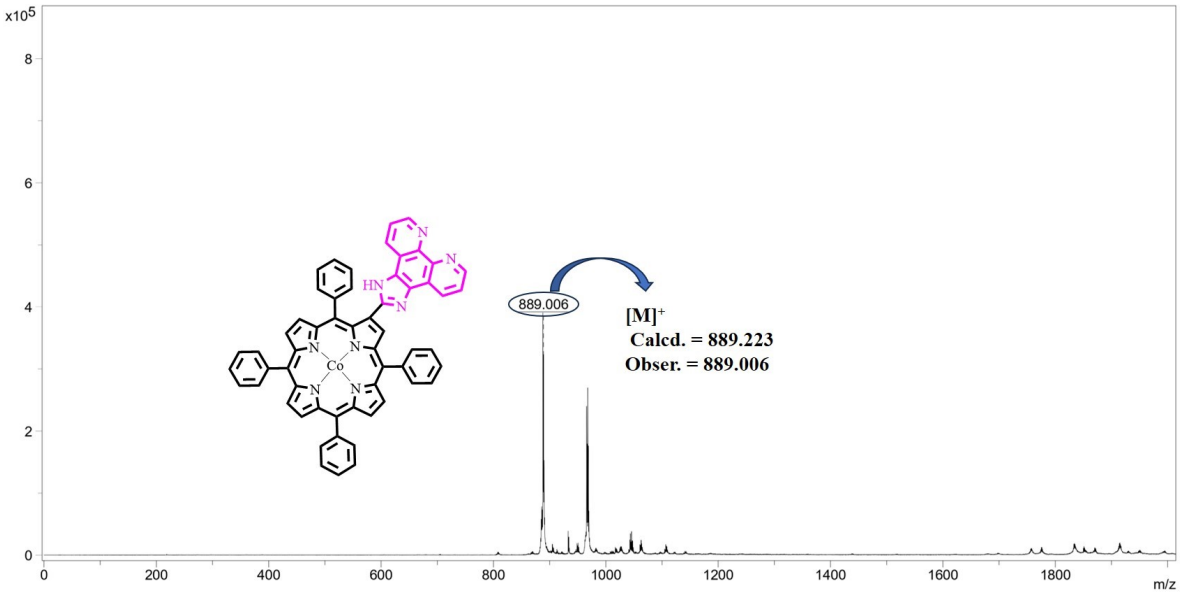

Fig. S3. MALDI-TOF mass spectrum of CoTPP(Phen) with HABA matrix in positive ion mode at 298 K.

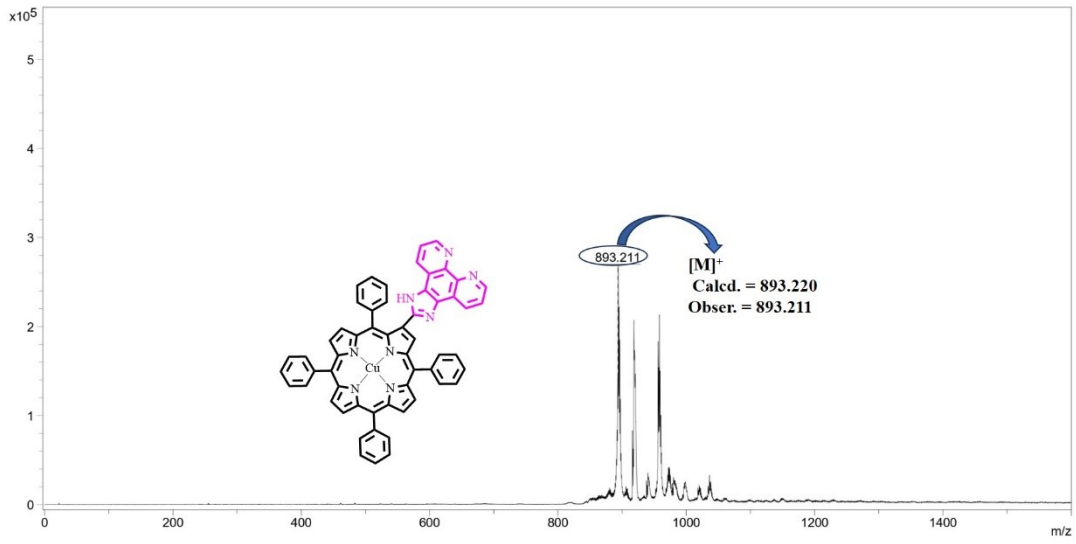

Fig. S4. MALDI-TOF mass spectrum of CuTPP(Phen) with HABA matrix in positive ion mode at 298 K.

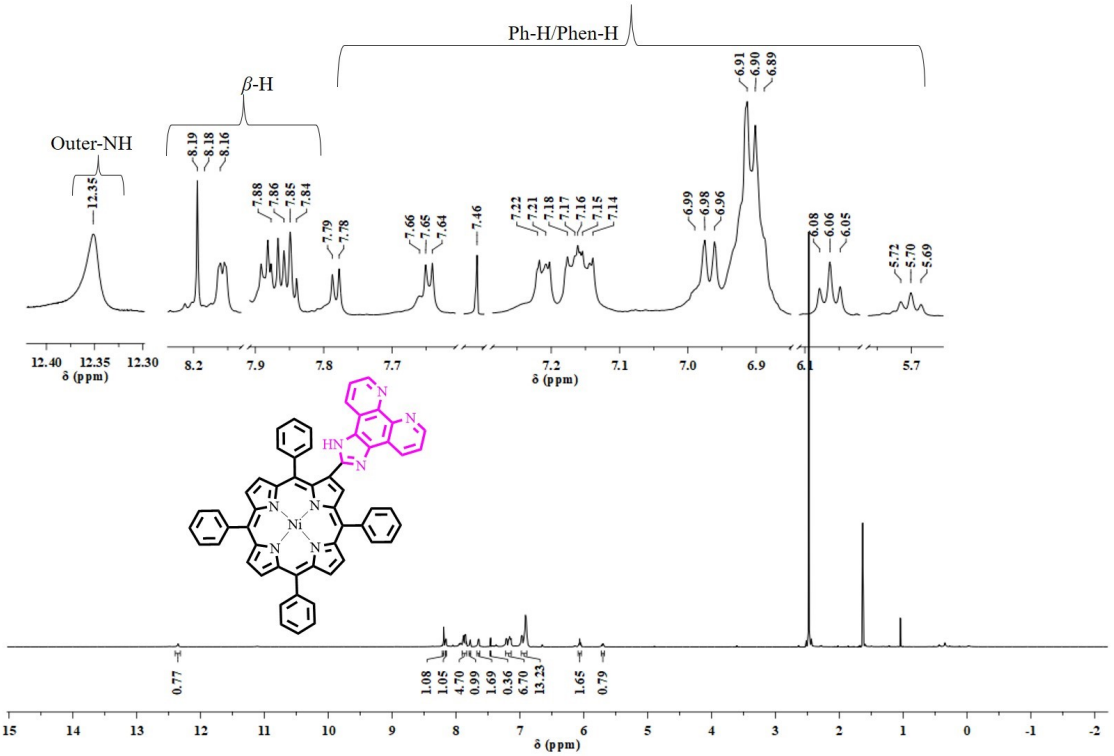

Fig. S5. ^{1}H NMR spectrum of NiTPP(Phen) in DMSO-d_6 at 298 K.

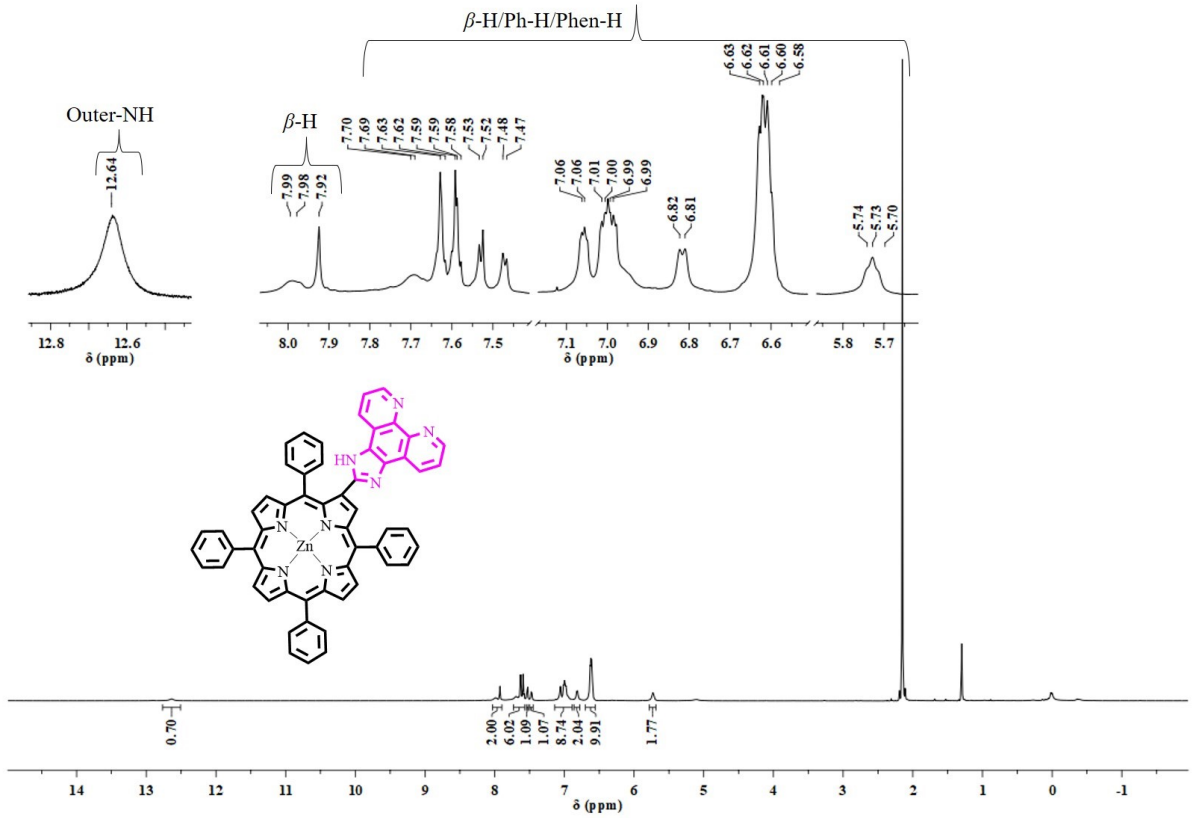

Fig. S6. ^{1}H NMR spectrum of ZnTPP(Phen) in DMSO-d_6 at 298 K.

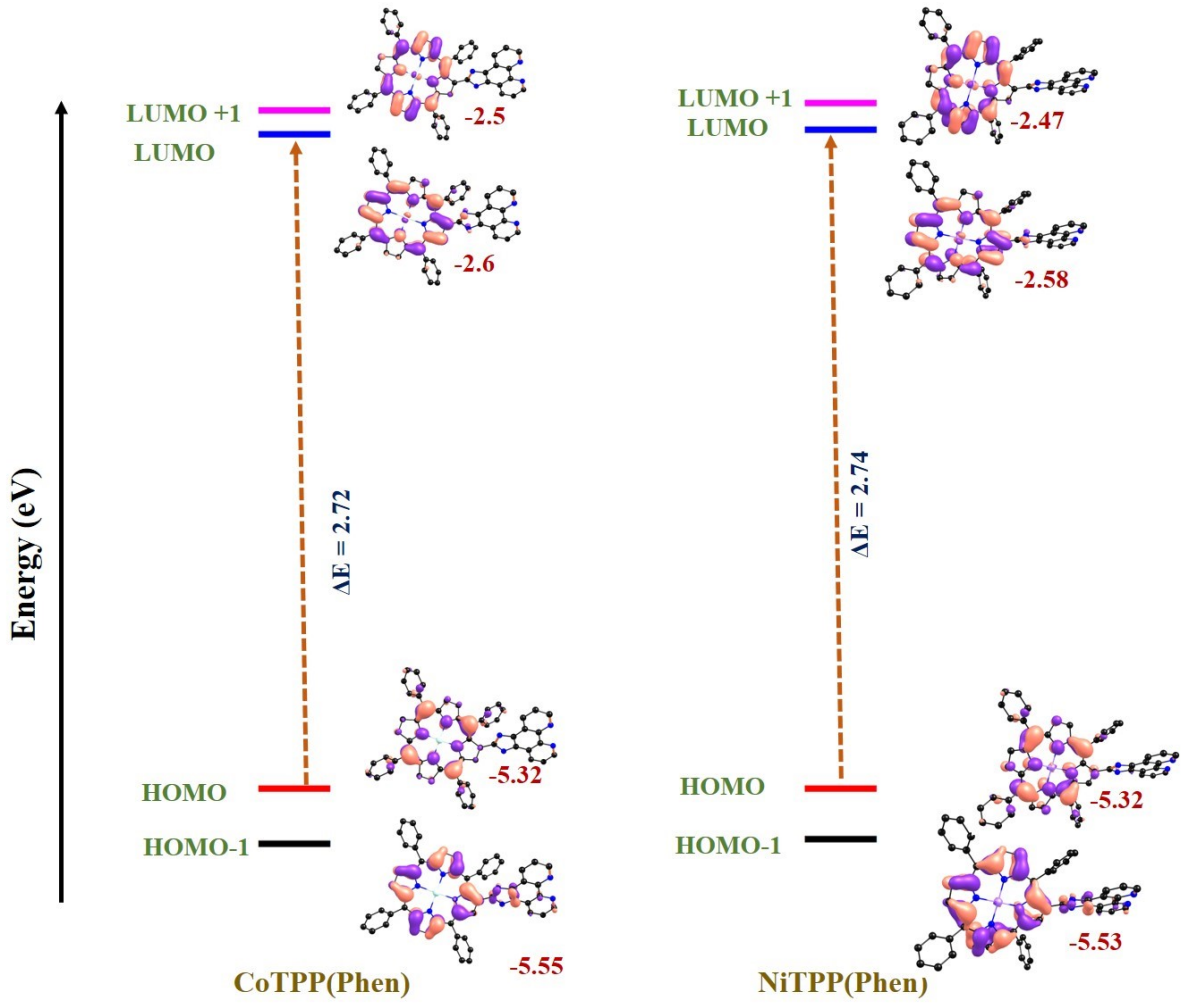

Fig. S7. Energy profile depicting frontier molecular orbitals for MTPP(Phen) (M = Co, Ni).

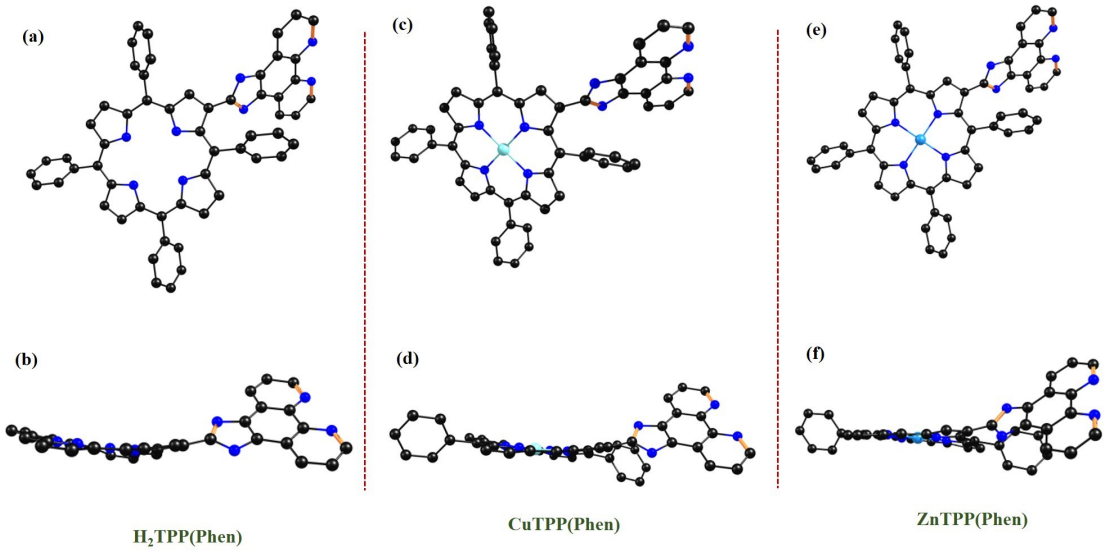

Fig. S8. Ground state optimized geometries showing top views of (a) H_2TPP(Phen), (c) CuTPP(Phen), (e) ZnTPP(Phen) side view (b) of H_2TPP(Phen), (d) CuTPP(Phen), (f) ZnTPP(Phen) (*meso*-phenyl has been removed for clarity in the side view).

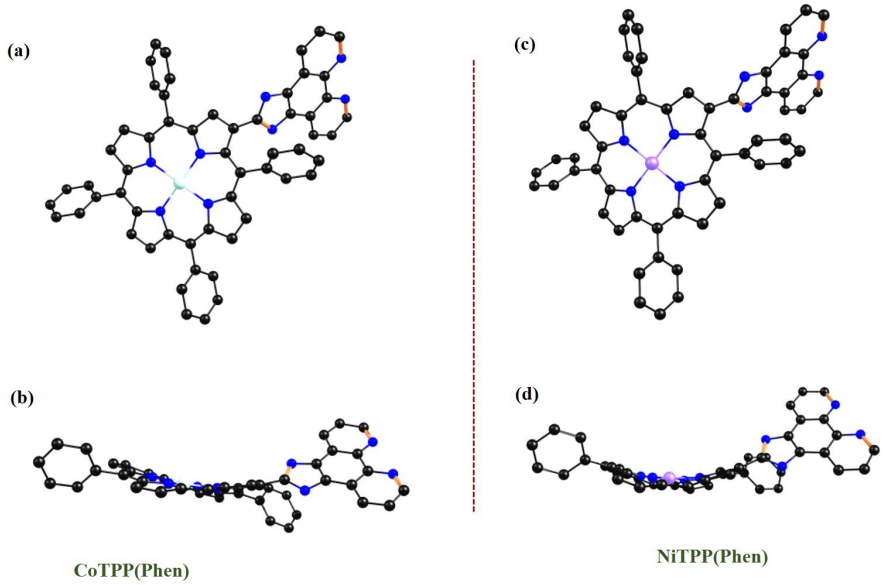

Fig. S9. Ground state optimized geometries showing top views of (a) CoTPP(Phen), (c) NiTPP(Phen), side view (b) of CoTPP(Phen), (d) NiTPP(Phen) (*meso*-phenyl has been removed for clarity in the side view).

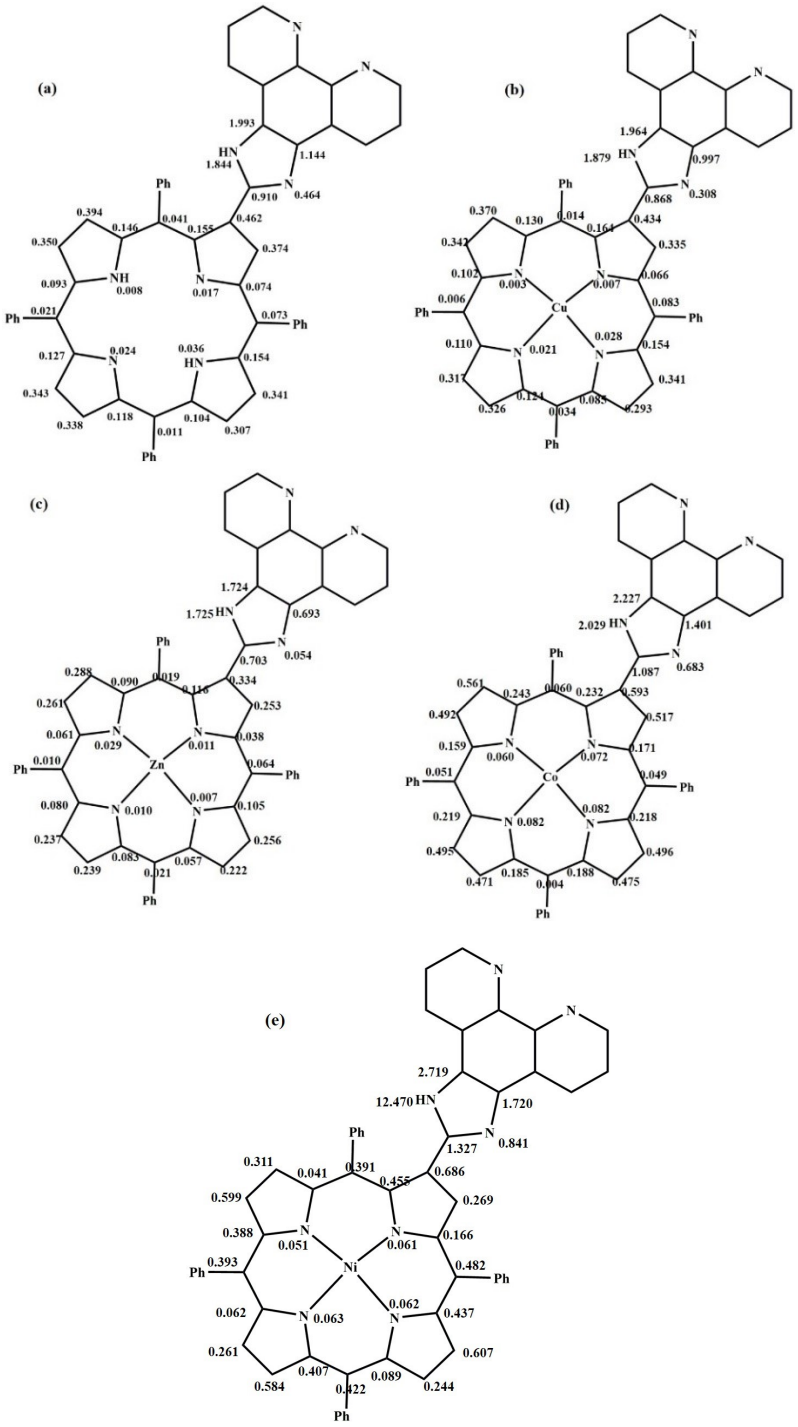

Fig. S10. Displacement of 24-core atoms of porphyrin from mean plane of (a) H_2TPP(Phen), (b) CuTPP(Phen), (c) ZnTPP(Phen), (d) CoPP(Phen), and (e) NiTPP(Phen).

Table S1. Selected bond lengths (Å) and bond angles (º) of H_2TPP(Phen), H_2OPP(Phen), VOTPP(Phen), and VOOPP(Phen).

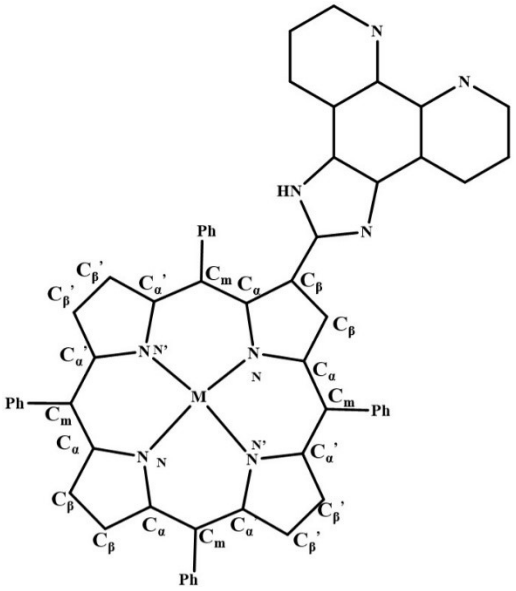

M = H_2, Ni, Cu, Co, Zn

	H_2TPP(Phen)	CuTPP(Phen)	NiTPP(Phen)	ZnTPP(Phen)	CoTPP(Phen)
Bond Length (Å)					
M-N		2.036	1.960	2.077	1.991
M-N'		2.024	1.953	2.065	1.985
C_β-C_β	1.365	1.375	1.377	1.378	1.375
C_β'-C_β'	1.373	1.371	1.370	1.373	1.370
N-C_α	1.382	1.397	1.399	1.395	1.400
N-$C_{\alpha'}$	1.386	1.397	1.398	1.396	1.400
C_α-C_β	1.464	1.454	1.451	1.457	1.451
C_α'-$C_{\beta'}$	1.439	1.454	1.452	1.457	1.452
C_α-C_m	1.412	1.409	1.403	1.417	1.404
C_α'-C_m	1.406	1.407	1.402	1.416	1.403
ΔC_β	0.363	0.344	0.445	0.261	0.512

Δ24	0.171	0.163	0.313	0.120	0.257
Bond Angle (°)					
M-N-C_{α}		126.505	126.92	126.12	126.967
M-N'-$C_{\alpha'}$		126.56	126.985	126.227	126.987
N-M-N		178.32	176.49	179.56	175.64
N'-M-N'		180.00	176.57	179.71	175.83
N-C_{α}-C_{m}	125.73	126	125.464	125.825	125.635
N'-C_{α}'-C_{m}	126.85	126.415	125.857	126.262	125.987
N-C_{α}-C_{β}	110.09	109.465	109.912	108.937	109.962
N'-C_{α}'-C_{β}'	106.30	109.602	110.047	109.07	110.092
C_{β}-C_{α}-C_{m}	124.13	124.487	124.247	125.21	124.285
C_{β}'-C_{α}'-C_{m}	126.83	123.972	123.89	124.67	123.855
C_{α}-C_{m}-C_{α}'	124.87	123.075	120.937	124.672	121.872
C_{α}-C_{β}-C_{β}	106.75	107.23	107.08	107.352	107.125
C_{α}'-C_{β}'-C_{β}'	108.35	107.265	107.122	107.385	107.152
C_{α}-N-C_{α}	106.20	106.495	105.50	107.34	105.52
C_{α}'-N-C_{α}'	110.65	106.22	105.685	107.06	105.35